Study of the behavior of low voltage ZnO varistors against very fast transient overvoltages (VFTO)

Clara Rojo Ceballos, Farid Chejne [*], Ernesto Pérez, Andrés Osorio, Alexander Correa

Universidad Nacional de Colombia, Facultad de Minas, Carrera 80 No. 65-223, Medellín, Colombia

ARTICLE INFO

ABSTRACT

To study the behavior of low voltage ZnO varistors against Very Fast Transient Overvoltage (VFTO), the authors have developed a complete VFTO(s) generation and measurement system based on magnetic pulse compression (MPC) and Transmission Line Transformer (TLT). This system has an output voltage of 24 kV, rise time of 32 ns, and a bandwidth of 10 MHz. The measurement system comprises a damped resistive voltage divider with an impedance of 1000 MΩ and a maximum bandwidth of 10 MHz.

The experiment was performed with five commercial zinc oxide varistors with a nominal voltage of 150 V, each one was subjected to VFTO-type voltage pulses and, by Analysis of Variance (ANOVA), a single varistor was selected to perform the case study.

This work presents an experimental methodology to observe the response of low voltage ZnO varistors against VFTO. This response is the delay of the residual voltage to the applied discharge current and indicates the poor performance of these devices against VFTOs. Our methodological proposal consists of a series of laboratory tests that will allow manufacturers and consumers to take corrective measures in case of malfunction, damage of the varistor material, or permanent degradation of the device.

1. Introduction

The Gas Insulated Substations (GIS) have gained acceptance among the power utilities due to their easy maintenance, requirement of less space, high reliability, and good environmental adaptability. Even though the gas-insulated substations are more reliable than the traditional air-insulated substations, the switching operations in them can lead to Very Fast Transient Overvoltages (VFTOs), which in turn affect the dielectric strength of insulation of the equipment connected in the substation [1].

The waveform of VFTOs has a short rise time and a large amplitude; such parameters clearly describe this type of transient voltages. However, the configuration and parameters associated with the gas-encapsulated substations also determine the rise time and the oscillation frequency of the VFTOs' waveform, which can reach values from 0.5 to 150 MHz [2,3].

The field test could directly provide the waveform and allow to analyze its characteristics, but it has not been standardized for VFTO neither in engineering nor in the academic field [4–8].

Most of the research conducted to evaluate the characteristics of VFTOs and their influence on the performance of a metal oxide arrester are based on the data collected in GIS during switching operations [9–11]. Other research used substation models on specialized software [12–15], which have derived also on equivalent GIS circuits using transmission line theory and Thevenin's theorem [16].

To avoid insulation failure of equipment in gas-enclosed substations, the level of insulation must be greater than the magnitude of the transient overvoltages that may occur in it. These overvoltages are usually limited to an acceptable level of protection by employing devices such as metal oxide arresters, which have been used for over 25 years in power systems. Therefore, researchers have a wide interest in the analysis of the dynamic behavior against transient currents [9], the potential distribution in the varistor column [10], and the effect of self and parasitic capacitances associated with the arrester [11].

These devices are made of varistor blocks that use metal oxide materials that modify their conductive behavior against the electric field [12]. Typically, small blocks are used for low voltage applications and series arrangements for high voltage.

Several electrical models with acceptable levels of accuracy have been used to simulate its frequency-dependent behavior under current
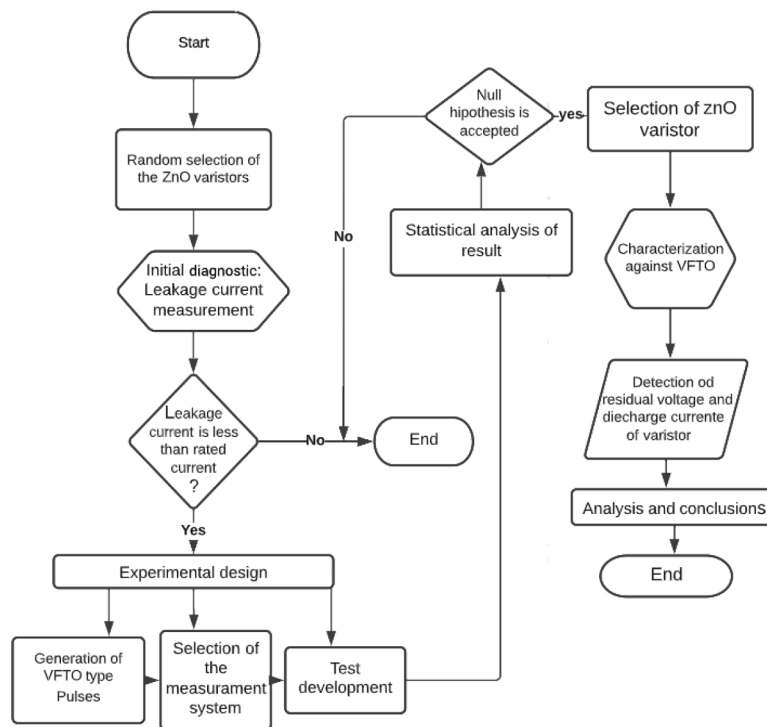
Fig. 1. Methodological structure of the characterization of low-voltage ZnO varistors against VFTO.

surges with a front time of 1 μs or more [13–18]. For high-frequency current surges, there is a delay between the peaks of residual voltage and the discharge current due to the capacitance effect [19].

No studies have been reported in the literature on the characterization of low-voltage ZnO varistors in VFTO based on laboratory tests, where the applied voltage is generated by a device whose output signal meets the characteristics of a VFTO-type voltage transient, such as a short rise time, a large amplitude and a frequency in the MHz range.

The objective of this study is to analyze the behavior of low voltage varistors under non-standard oscillatory type current pulses by laboratory tests using a high voltage pulse generator designed based on magnetic pulse compression (MPC) and transmission line transformers (TLT).

In this study, the delay between the residual voltage and the discharge current in a low-voltage ZnO varistor before VFTO transients is detected by means of laboratory tests; the methodology based on tests used in this work can be useful for manufacturers, who should take corrective actions regarding the selection of the varistor material, or consider the addition of special elements and improvement of the sintering process to reduce the capacitive effect and thus improve the performance of conventional varistors.

2. Equipment, materials, and methods

The general structure of the research aimed at the characterization of low-voltage ZnO varistors is presented in Fig. 1, which contemplates the step-by-step process carried out.

2.1. Equipment: high voltage pulse generator

In this study, a high voltage pulse generator is used with a maximum output voltage signal of 32 kV and a rise time of 40.5 ns at a maximum frequency of 10 MHz.

Fig. 2 shows the equivalent circuit of the high-voltage pulse generator, which delivers a non-standardized voltage signal associated with these VFTOs. This system consists of a primary capacitor (Cp), two electromechanical automation systems that allow charging and

discharging the primary capacitor (R_1, R_2), (PT). A high couple efficiency pulse transformer was adopted to reduce the charging time from Cp to C_1, (L_1, L_2, L_3), saturable inductors, capacitors (C_1, C_2, C_3), high voltage coaxial cables (L $_{Line\ 1}$, L $_{Line\ 2}$, L $_{Line\ 3}$), and the load being the ZnO varistor under test (Z_L).

The process of magnetic compression of the initial voltage pulse is the following: when the switches are closed, C_1 is loaded by the pulse transformer (PT). If the voltage on C_1 (V_{C1}) reaches its maximum value, L_1 saturates and allows C_2 to be charged. Similarly, inductors L_2 and L_3 saturate sequentially and a rise time of the order of ns is obtained.

The TLT technology offers a high frequency response compared to other types of high voltage pulse generators; in this case, by using three coaxial cables the frequency is limited to only 10 MHz.

2.2. Digital oscilloscope

An oscilloscope with a bandwidth of 200 MHz, a maximum sampling rate of 2.5 GS/s, and a voltage ratio of 1:1000 is used to detect residual voltage and discharge current.

2.3. Test sample

For the experiment, five commercial ZnO varistors with a nominal voltage of 150 V and a maximum current type 8/20 μs of 40 kA were randomly selected. Since there were no records of the experiment to be performed, a varistor was subjected to 7 applications of VFTO type voltage pulses to establish an initial descriptive statistic, which is presented in Table 1. These data allowed us to establish the maximum number of repetitions per varistor necessary in the experiment.

The results of the descriptive statistics show that the mean, median, and mode are approximately equal, being the standard error 0.6% of the value of the mean. Thus, it is possible to infer that these results follow a normal distribution, and we decided to decrease the standard error to 0.2%, increasing by 20 the number of interferences in the test [21].
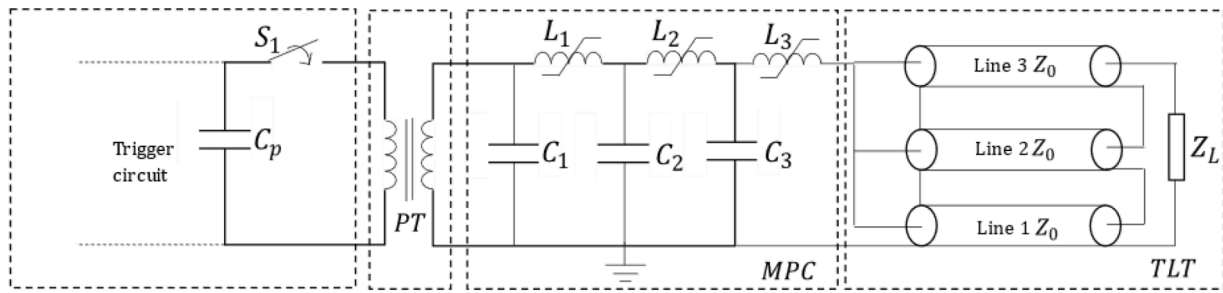
(a)
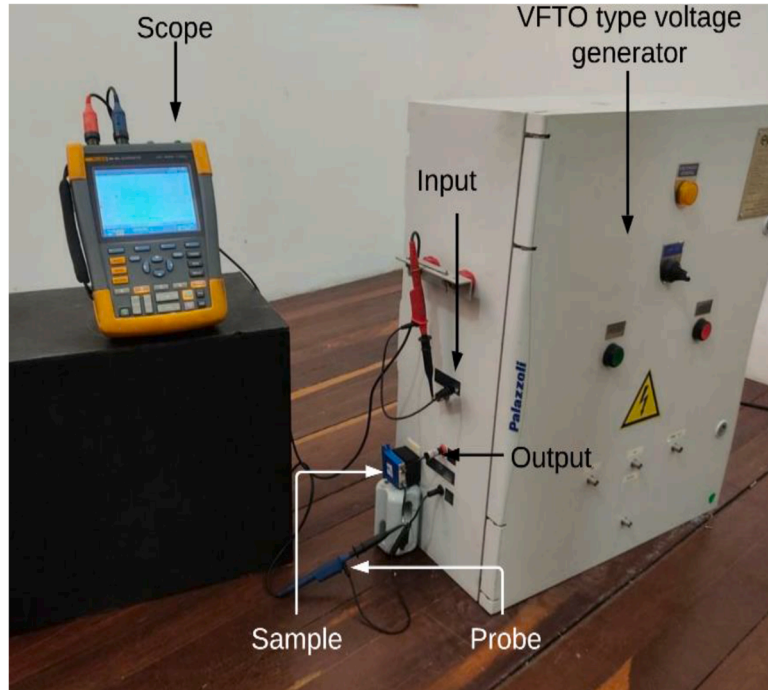
(b)

Fig. 2. High voltage pulse generator: (a) Internal circuit diagram modified from VFTO type voltage pulse generator [20]; (b) Experimental and measurement setup.

Table 1
Descriptive statistics.

Replica	Residual voltage [V]	Descriptive Statistics [V]	
1	15,984,37	Average	15,630.72
2	15,993,75	Typical error	95,47
3	15,643,75	Median	15,648.43
4	15,653,12	Mode	15,653,12
5	15,878,12	Standard deviation	
6	15,384,37	287.75	
7	15,231,25		

2.4. Methodology

The methodology applied includes the following steps:

2.4.1. Validation of the voltage pulse waveform at the generator terminals without load

The Electromagnetic Transients Program (ATP/EMTP) is used to validate the experimental waveform. The models of some apparatus in the experiment are shown in Table. 2.

For the simulation, the Line Constants routine is used to obtain the traveling wave model.

The following is the ATP model of the VFTO signal generator resulting from the MPC and TLT junction

In the experimental waveform presented in Fig. 2(a), three zones characterized by their magnitude and frequency range can be established. Zone I has a magnitude of 15.3 kV and a dominant frequency around 7.91 MHz; it was chosen to carry out this study.

Zone II presents a maximum voltage of 5.42 kV and frequency components of the order of 7.88 and 31.52 MHz. Zones III and IV are dominated by high magnitude voltages, but with low frequency components of the order of 1.92 MHz; therefore, they are not considered in this study.

Comparisons of the transient waveform of the experimental voltage signal with that obtained in the simulation presented in Fig. 2 show that the basic oscillation frequency of the simulation agrees with that obtained in the laboratory.

There is a deviation in magnitude and rise time of 0.5 and 0.85 ns between the two signals, respectively, so that a good approximation can be established between the experimental and the simulated voltage signal.

Table 2

Models used in ATP simulation For the simulation, the Line Constants routine is used to obtain the traveling wave model.
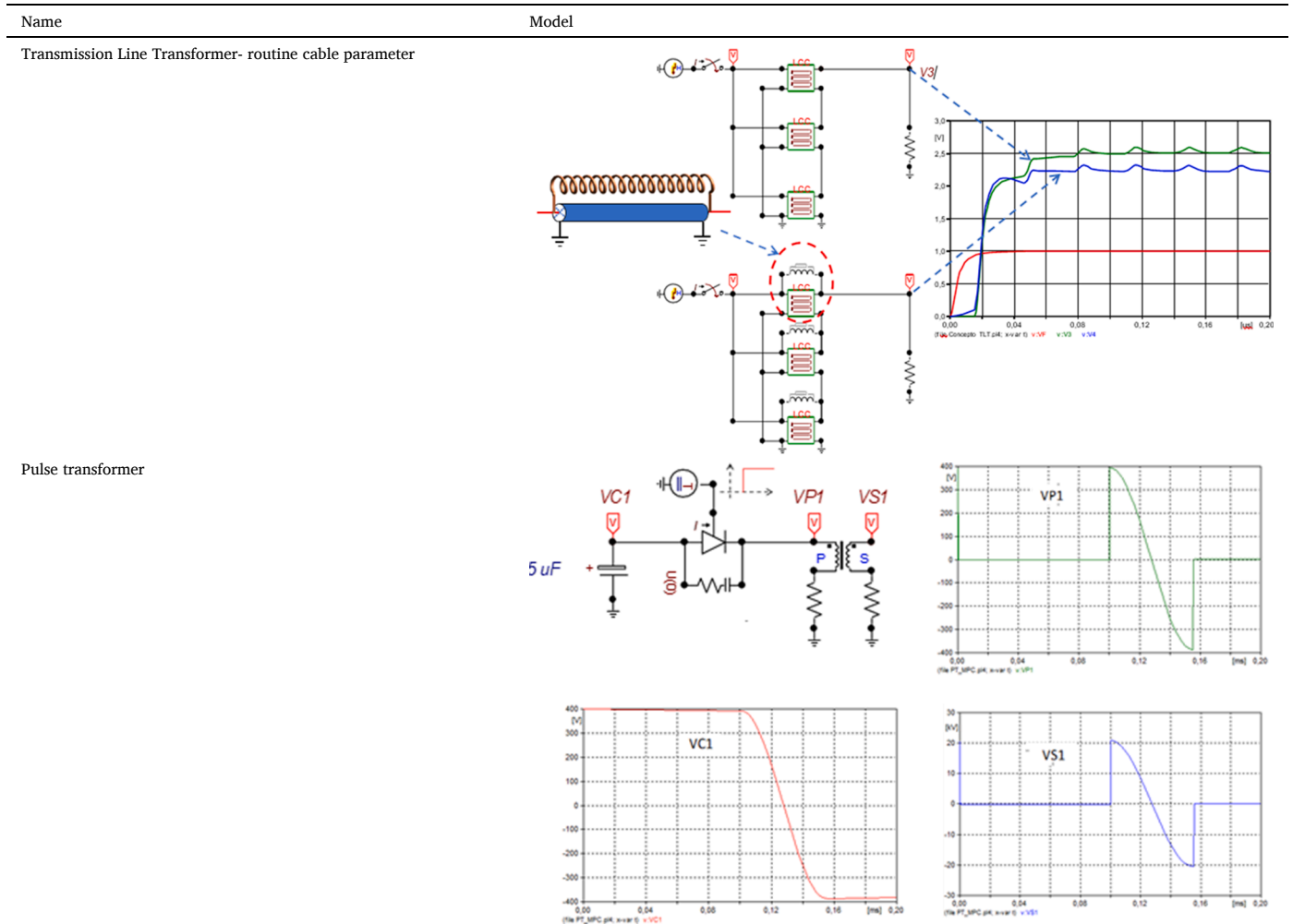
Name	Model
Transmission Line Transformer- routine cable parameter	
Pulse transformer	

Table 3

Parameters of the experimental and simulated VFTO type voltage waveforms.

Waveform	Input voltage [kV]	Output Peak voltage [kV]	Rise Time [ns]
Experimental	0,22	32	40,5
Simulated in ATP	0,22	31	42,2
Deviation		0,5	0,85

Table 4

Leakage current values of the five varistors.

Leakage current [mA]	Varistor 1	Varistor 2	Varistor 3	Varistor 4	Varistor 5
	0.22	0.225	0.22	0.219	0.223
Average [mA]	0.22175	Deviation [mA]	0.0027		

2.4.2. Initial diagnosis of ZnO varistors

The leakage current at rated voltage is measured at the five varistors to establish their initial condition prior to testing in the laboratory. The values obtained are presented in Table 3.

The maximum leakage current established by the varistor manufacturer is 0.30 mA. Due to the above, the good condition of the five ZnO varistors can be accepted before submitting them to laboratory tests.

2.4.3. Varistors testing at the high voltage laboratory

The equivalent circuit of the residual voltage and discharge current test of the ZnO varistors is shown in Fig. 3. These parameters were recorded with a digital oscilloscope using a damped resistive divider with a transformation ratio of 20 kV/200 V and a 20mΩ resistive shunt, respectively. The performance of the damped resistive divider for high frequencies is presented in Fig. 4, which is compared with the behavior of a resistive divider for the same applied signal. This figure shows that the transformation ratio of the damped resistive divider remains constant up to a frequency of 10 MHz, which makes it suitable for measuring the residual voltage of the ZnO varistors under test.

2.4.4. Statistical analysis of results

An Analysis of Variance (ANOVA) is performed to establish the variability of results of the residual voltage and discharge current of the five varistors under test. It also allows us to select a single varistor with the smallest deviation in data and to characterize it against VFTO type voltage pulses.
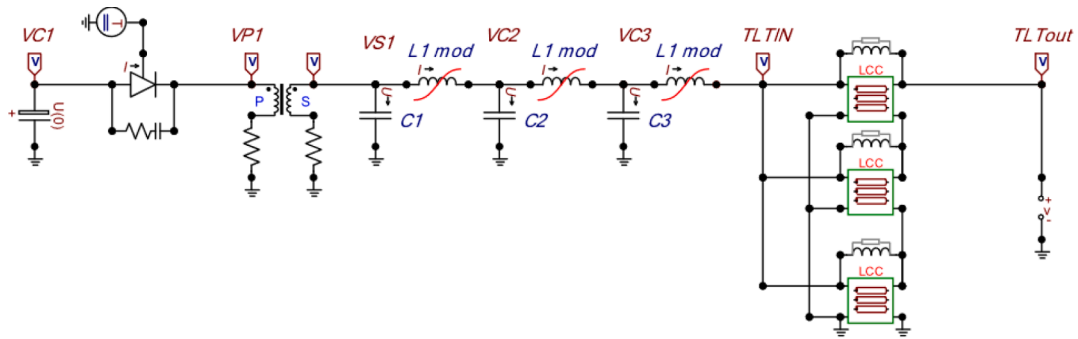
Initially, it is necessary to establish the factor under study, its possible levels, and the null and alternative hypotheses.
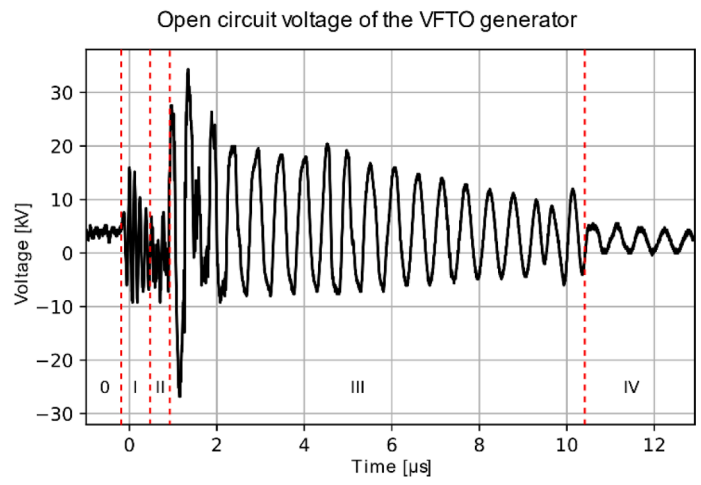
Factor: Varistor

Level: 1,2,3,4,5 (number of varistors under study)

The hypotheses put forward in this analysis are the following:
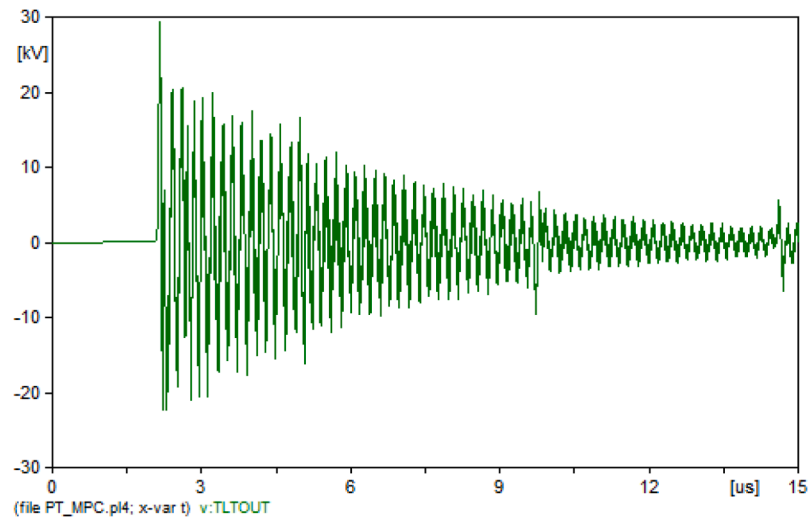
Null hypothesis: $H_o : \mu_1 = \mu_2 = \mu_3 = \mu_4 = \mu_5$.

(a)

(b)

(c)

Fig. 3. a) Circuit used in the simulation; b) Open circuit voltage waveform associated with the VFTO type voltage pulse generator; c) Voltage waveform obtained with The Electromagnetic Transient Program (ATP/EMTP).
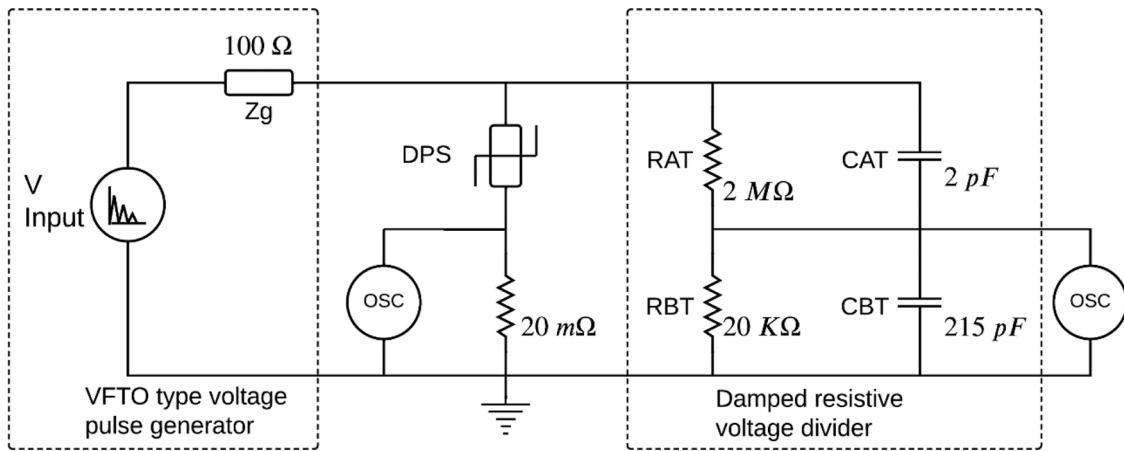
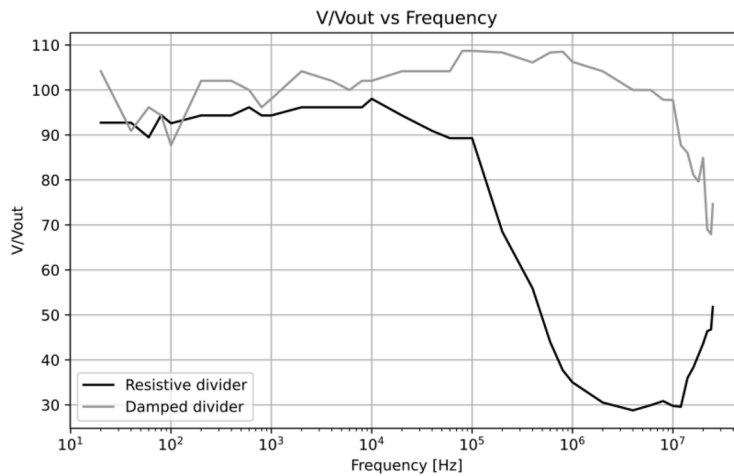Fig. 4. Equivalent circuit of the residual voltage and discharge current measurement system in a ZnO varistor.

Fig. 5. Damped resistive divider response to different frequency values.

μ_j : mean value of residual voltage results and the discharge current of the five varistors under test for $j = 1, 2, 3, 4, 5$

The mean values of the residual voltages and discharge currents of the five selected varistors do not present statistically significant differences.

Alternative hypothesis H_1: At least one of the means of the values of the residual voltage and the discharge current of the five varistors presents statistically significant differences.

The analysis of variance (ANOVA) is a parametric hypothesis test and assumes that the residual voltage and discharge current data follow a normal distribution, so the parametric criteria must be checked in the obtained results, these are presented in the results section.

3. Results and discussion

3.1. Statistical analysis of experimental results

3.1.1. Analysis of variance of experimental results

The typical residual voltage and discharge current waveform are presented in Fig. 5.

The front time of the voltage and current waves were defined as the duration between zero seconds and the time to reach the peak value, these times are around 22 and 40 ns, respectively.

The variability of tests results is presented in Fig. 6, the average values of the discharge current and residual voltage of each varistor were taken.

Table 5 shows the values of the discharge current of the five ZnO varistors, and Table 6 shows the values of the residual voltage of the five ZnO varistors.

Those values were subjected to the Analysis of Variance (ANOVA) for a significance level of 5% (δ) using the MINITAB 21 software, and the following results were obtained.

Model Summary

R square

S R square fitted

376.9 32.72% 29.88%

$S = 376,9$, R-squ (R^2). = 32,72%, R-cuad.(fitt) = 29,88%

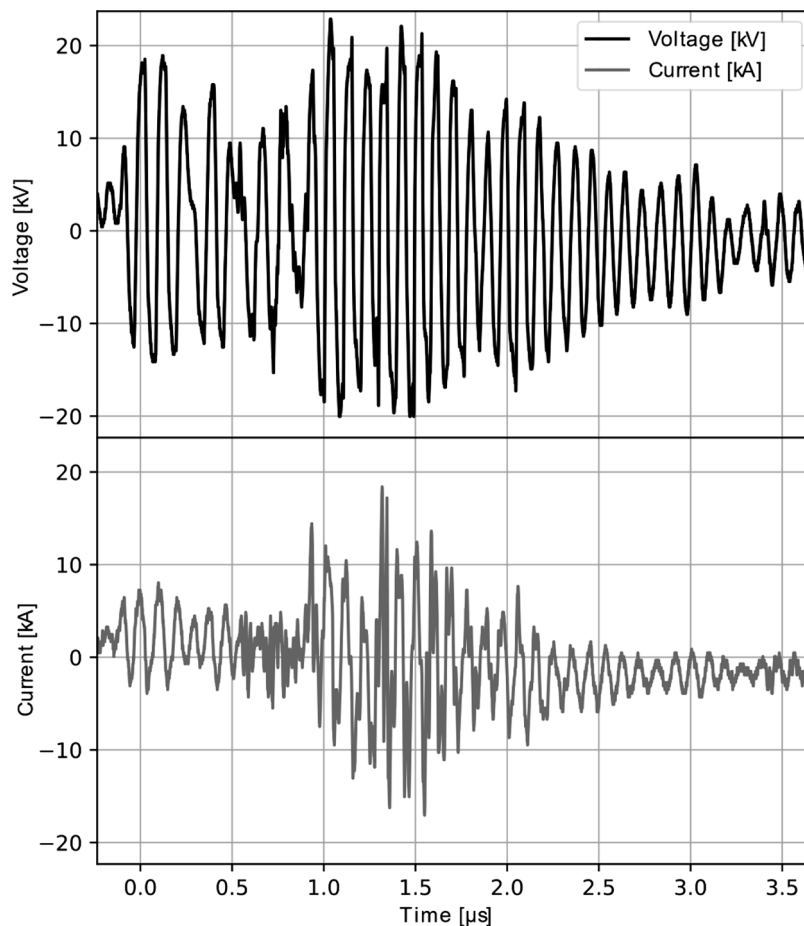R^2 : 32.7 is the percentage of variation in the response, explained by

Fig. 6. Waveform of residual voltage and discharge current of ZnO varistors under test.

Table 5
Experimental values of the discharge current of the five ZnO varistors.

Discharge current (A) Varistor 1	Discharge current (A) Varistor 2	Discharge current (A) Varistor 3	Discharge current (A) Varistor 4	Discharge current (A) Varistor 5
5467,18	6715,6	6575	5996,88	5929,69
5332,81	6821,8	6762,5	6000	6462,5
5539,06	6623,44	6132,81	6056,25	5984,38
5703,12	6607,81	5942,19	6092,19	5914,06
5859,37	6459,38	5932,81	6765,63	6828,13
5887,5	6059,38	5760,94	7470,31	5760,94
5531,25	6310,94	5884,38	6557,81	5878,13
6251,56	5871,88	6473,44	5992,69	6754,69
5914,06	5796,6	6604,69	6462,5	7262,5
5534,37	6032,1	6331,25	5984,38	7470,31
5718,75	6126,56	6012,5	5914,06	6557,81
5803,12	6404,69	5982,81	6828,13	6204,69
5223,43	6190,6	6092,19	5760,94	6300
5831,25	5962,5	5892,19	5878,13	6682,81
5421,87	5992,19	6146,88	6754,69	6443,76
5689,06	6360,94	6326,56	7262,5	5996,88
5968,75	6264,99	6362,5	6204,69	6000
5625	6570,31	5434,38	6300	6056,25
5428,12	6059,38	6204,69	6682,81	6092,19
5896,87	6068,75	5771,88	6443,75	6765,62

Table 6
Experimental values of the residual voltage of the five ZnO varistors.

Max Voltage varistor 1	Max Voltage varistor 2	Max Voltage varistor 3	Max Voltage varistor 4	Max Voltage varistor 5
11,362,5	18,046,88	15,515,63	15,678,13	15,231,25
13,162,5	18,150	14,850	15,550	15,653,13
12,368,75	17,771,88	15,218,75	15,137,5	17,518,75
13,468,75	14,303,13	14,878,13	16,315,63	16,893,75
13,784,38	15,096,88	14,540,63	14,556,25	14,925.00
14,640,63	16,412,5	12,531,25	15,368,75	16,012,5
15,371,88	14,068,75	14,893,75	15,515,63	15,112,5
13,662,5	14,250	15,196,88	15,315,63	15,171,88
14,353,13	12,340,63	14,900	15,806,25	15,828,13
13,256,25	14,121,88	15,121,88	15,240,63	16,984,38
12,096,88	15,721,88	14,975	15,940,63	17,284,38
13,837,5	14,075	14,750	14,525	15,984,38
13,865,63	16,821,88	14,912,5	17,293,75	15,993,75
13,725	12,865,63	14,115,63	16,043,75	15,643,75
13,843,75	14,259,38	15,918,75	16,384,38	15,653,13
15,678,13	16,868,75	17,212,5	15,762,5	15,878,13
12,893,75	13,437,5	14,753,13	15,696,88	15,384,38
13,346,88	13,800	14,543,75	16,084,38	14,990,63
11,031,25	14,353,13	15,221,88	15,606,25	18,193,75
14,362,5	15,971,88	14,712,5	14,328,13	19,443,75

Table 7
Unidirectional ANOVA: Residual voltage VS Varistor.

Source	GL	SC	MC	F	p
Varistor	4	80203834	20050959	14,41	0,00
statistical error	95	132172240	1391287		
Total	99	212376075			

GL: Degrees of freedom, SC: Sum of Squares, MC: Mean of squares, F: Test statistic used to determine whether the term is associated with the response, and P: Probability to measure the evidence against the null hypothesis.

Table 8
Dispersion of the residual voltage results.

level	N	Mean	Standard deviation
1	20	13506	1170
2	20	15137	1729
3	20	14938	848
4	20	15608	687
5	20	16189	1186

Individual 95% confidence intervals
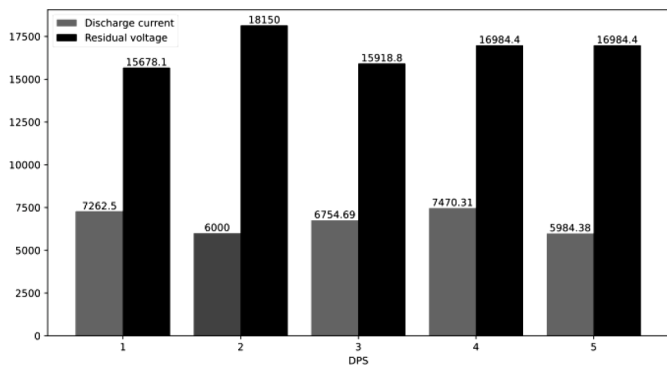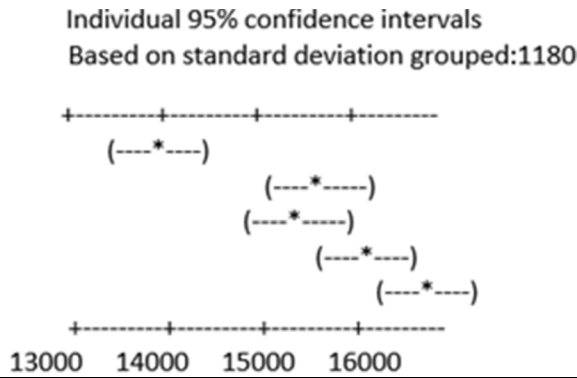Based on standard deviation grouped:1180

Fig. 7. Variability of the maximum values of the residual voltage and discharge current of the varistors under test.

Table 9
Results of Tukey's test.

Varistor	N	Mean	Grouping
5	20	16,189	A
4	20	15,608	AB
3	20	15,137	B
2	20	14,918	B
1	20	13,506	C

the model.

Interpretation.

$P < \delta$, this is $0.000 < 0.005$. Therefore, the null hypothesis is rejected, or it can be established that some of the varistors have different mean values.

The following analysis allows us to know which varistor behaves differently in relation to the mean value of the residual voltage, establishing the confidence intervals for a probability of 95%.

The Table 8 shows a set of 95% confidence intervals

From Table 7 it can be established that varistor 4 has the smallest dispersion of the residual voltage results (687); varistor 1 presents a statistically significant difference because its confidence interval does not overlap with the confidence intervals of the others. This is verified with Tukey's test, which groups the information around the average value. The result show the formation of three groups of interest (A, B, C) and it is presented in Table 8. Group C corresponds to varistor 1, which is not taken into account for the study; it has no statistical relationship with varistors 2, 3, 4, and 5, as presented in Fig. 7.

In (a), varistor 1 has the lowest mean and varistors 4 and 5 have the highest. Varistors 2, 3, 4, and 5 have a similar behavior with respect to the mean. In (b), residuals vs. adjustments, the points appear to be randomly scattered on the graph. Neither group appears to have substantially different variability and there are no obvious outliers.

The studied varistor is chosen from the previous analysis of varistors 2, 3, 4 and 5, thus obtaining the results presented below.

Interpretation

$P < \delta$, this is $0.463 < 0.005$. Therefore, the null hypothesis is rejected, or it can be established that some of the varistors have different mean values.

Varistor 4, with the lowest standard deviation, is selected after analysis of the values on Table 9. The waveforms of the residual voltage and discharge current obtained during the tests, as well as the respective frequency spectrum, are presented in Figs. 7 and 8.

3.2. Waveforms of the residual voltage and discharge current pulse under load

Figs. 7 and 8 show very fast oscillatory non-standard waveforms of

Table 10
Unidirectional ANOVA: Discharge Current vs. Varistor (for varistors 2, 3, 4, 5).

Source	GL	SC	MC	F	P
Varistor	3	268260	89420	0.86	0.463
Statistical error	76	7859587	103416		
Total	79	8127847			

Table 11
Individual 95% confidence intervals Based on standard deviation Grouped: 376.9%.

level	n	Mean	Standard Deviation
2	20	6265	332,8
3	20	6131,3	329
4	20	6265,6	328,5
5	20	6264,6	331,7

```
                                              *............*...........*..........*
                                         (..........*.........)
                          (..........*.......)
                                                   (........*........)
                                                   (.......*.......)
               ..............*.............*.............*..............*
                         6000        6120        6240        6360
```
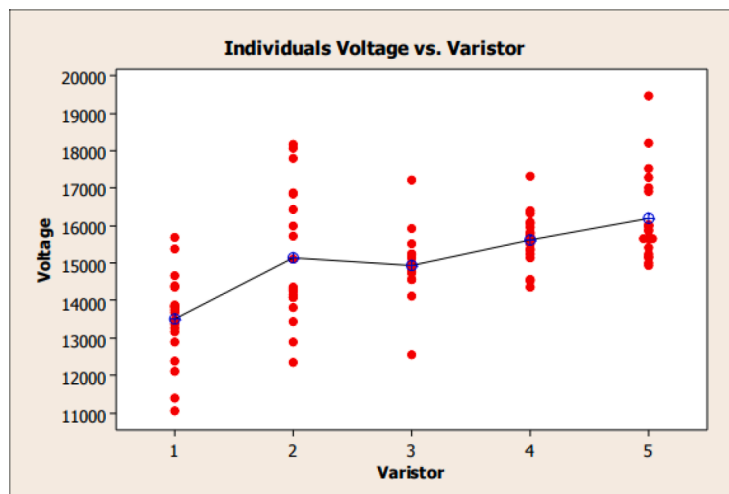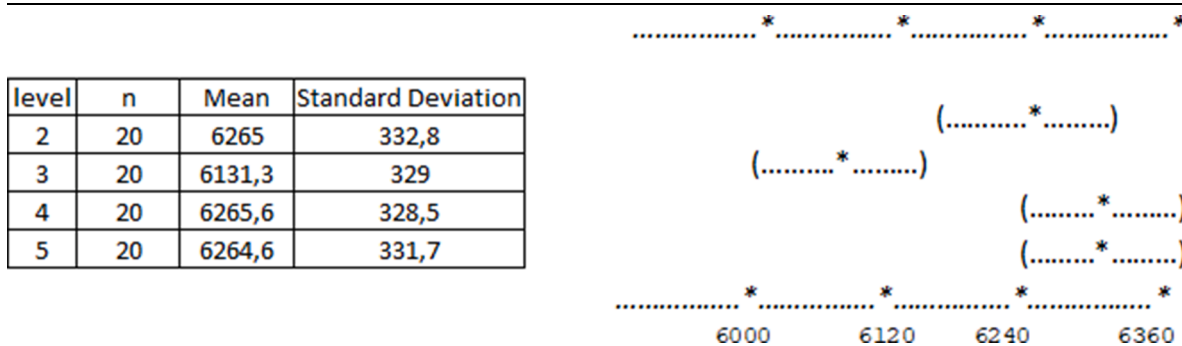

Fig. 8. Dispersion of residual voltage data for each varistor.

voltage and current for low voltage varistors when current impulse is injected by the generator.

The residual voltage and discharge current waveforms and their respective frequency spectra are illustrated in Figs. 8 and 9. The residual voltage reaches a maximum magnitude of 22 kV for a frequency of 10 MHz. This waveform is characterized by its damping and multi-frequency oscillations.

The charge current waveform reaches an amplitude of 17 kA for a frequency range of 10.8 MHz. The Fast Fourier transform is used to analyze the frequencies contained in the residual voltage and discharge current waveform obtained in the tests.

3.2.1. Characterization of low-voltage ZnO varistors against VFTO-type voltage transients

To understand the dynamic response of ZnO varistors to VFTOs, it is necessary to know the response of these devices to fast-front transients, where the discharge current has a rise time greater than 1.0 µs and the arrester reaches its peak value before the discharge current reaches its maximum, indicating that the varistor responds satisfactorily to this type of transient.

In the case study, a response of the varistor was obtained after the discharge current reaches its maximum value, as shown in Fig. 10.

The maximum value of the current is 7.5kAs with a rise time of 45 ns and a delay of 22 ns between the maximum value of the current and the
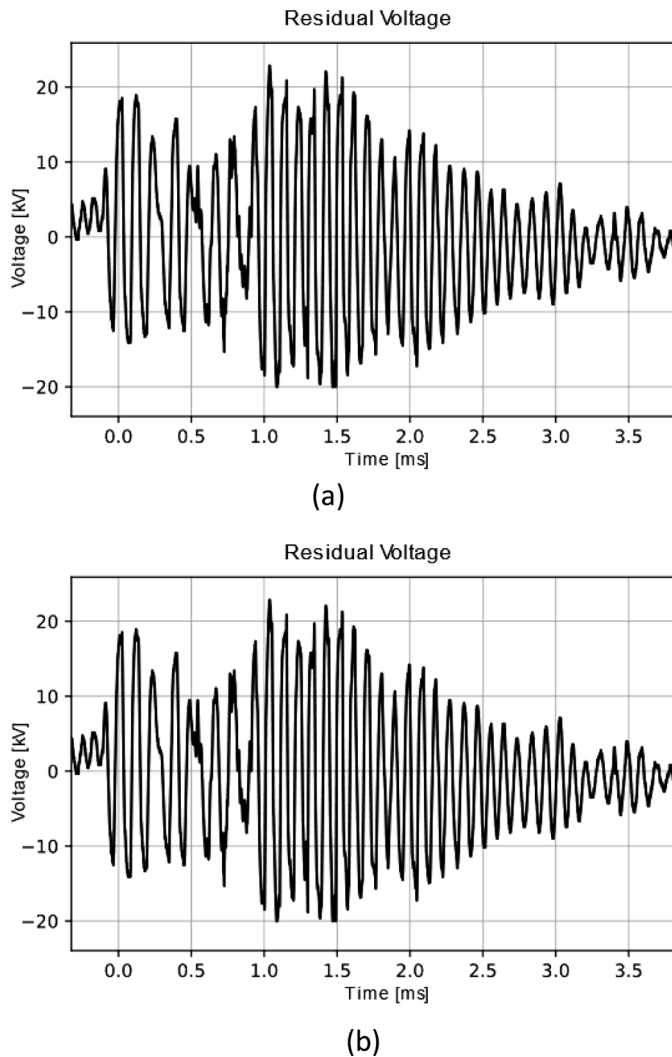
Fig. 9. (a) Waveform of the residual voltage at the terminals of the ZnO varistor; (b) Frequency spectrum.

peak value of the residual voltage. The maximum value reached by the residual voltage is 18 KV with a rise time of 34 ns.

The delay between the residual voltage and the discharge current applied to the varistor is due to two factors: the first is the rise time of the discharge current, which in the case of slow or fast overvoltages is of the order of μs and is enough for the varistor to pass from a capacitive state to a conducting state; the second is the stray capacitance and the associated with the system it is connected to.

4. Conclusions

To characterize the behavior of low-voltage ZnO varistors against oscillatory voltages with a very fast rise time, a VFTO pulse generator based on transmission line transformer and magnetic pulse compression technologies was designed and built with an output voltage of 32 kV and a damped oscillatory waveform with a rise time of 40.5 ns.

The simulated waveform of the generator's open circuit voltage is similar to the one obtained in the laboratory, with a difference of 1 kV in the peak values and 1.7 ns in the rise time. This can be due to the need for improving inductive coupling in the measurement system.
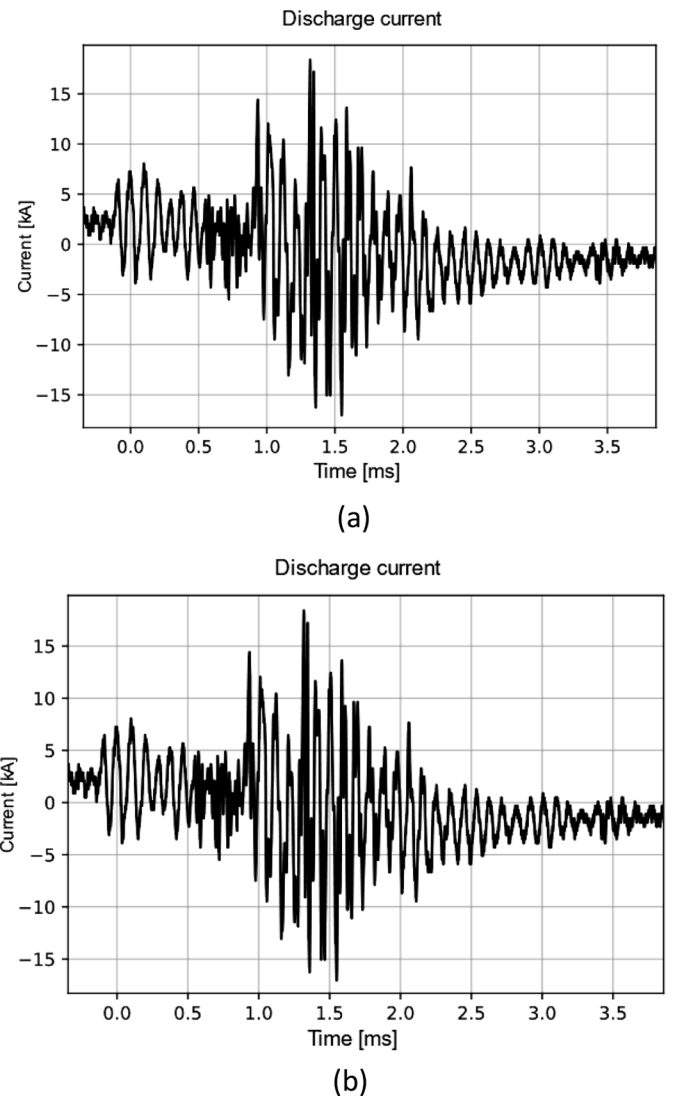

Fig. 10. a) Discharge current waveform with a magnitude; b) Frequency spectrum of 10 MHz.

In this research, a non-standard discharge current with a rise time of 45 ns less than 1μs was obtained, and the residual voltage in the sample peaks after the discharge current reached its maximum point, thus causing a delay in the varistor response. Therefore, it is important to estimate the actual rise time when studying the transient behavior of the varistor against the VFTO. The delay between the residual voltage and the discharge current is 22 ns, equivalent to an offset angle of 72°

The delay in the initial response time of the arrester may be one of the reasons for the failure of the arrester response in gas insulated substation when subjected to VFTO. Hence, it is essential to minimize the delay, as it indicates that the varistor does not conduct successfully in the presence of this type of pulses, and the switching from the capacitive state to the resistive state is slow.

CRediT authorship contribution statement

Clara Rojo Ceballos: Data curation, Writing – original draft, Software. **Farid Chejne:** Conceptualization, Methodology, Supervision. **Ernesto Pérez:** Conceptualization, Methodology, Supervision. **Andrés**
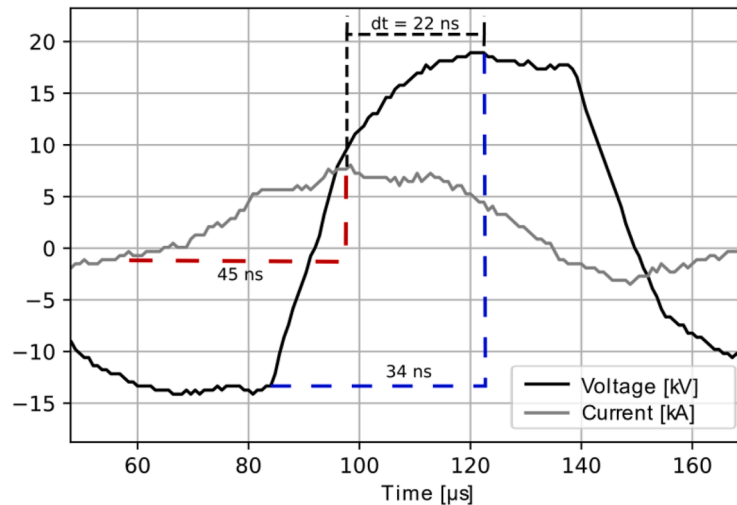
Fig. 11. Residual voltage of a ZnO varistor under test with a VFTO-type transient voltage.

Osorio: Software, Methodology. **Alexander Correa:** Visualization, Methodology.

Declaration of Competing Interest

The authors declare that they have no known competing financial interests or personal relationships that could have appeared to influence the work reported in this paper.

Data availability

No data was used for the research described in the article.

References

[1] U. Riechert and M. Szewczyk, "Mitigation of very fast transient overvoltages in gas insulated UHV substations CIGRE 2012 Mitigation of very fast transient Overvoltages in gas insulated UHV substations institute of power transmission and (DS) – Testing – bus-charging switching – very", no. July 2015, 2012.

[2] R.A. Almenweer, S. Yixin, and W. Xixiu, "Research on the fitting method to describe the mathematical expression of VFTO in GIS", vol. 2019, no. Acdc 2018, pp. 2053–2057, 2019.

[3] K. Prakasam, A. Pradesh, A. Pradesh, and E. Engineering, "International of electrical © I a E M E analysis of very fast transient over", vol. 6545, pp. 51–59, 2015.

[4] Y. Li, Y. Shang, L. Zhang, R. Shi, W. Shi, Analysis of very fast transient overvoltages (VFTO) from onsite measurements on 800kV GIS, IEEE Trans. Dielectr. Electr. Insul. 19 (6) (2012) 2102–2110.

[5] Y. Yu, W. Zanji, and S. Chong, "Determination of VFTO waveform in GIS according to simplified structure of GIS bus and circuit parameters", 2009 IEEE/PES Power Syst. Conf. Expo. PSCE 2009, pp. 1–9, 2009.

[6] K. Zhou, Y. Hu, H. Li, and F. Xue, "Time frequency characteristic analysis and simulation of VFTO waveform generated by disconnector switch in GIS", C. 2016 - Int. Conf. Cond. Monit. Diagnosis, pp. 194–197, 2016.

[7] I.-2019 60071-1, INTERNATIONAL STANDAR- . IEC 60071-1, 2020.

[8] S. Okabe, S. Yuasa, and S. Kaneko, "Evaluation of breakdown characteristics of gas insulated switchgears for non-standard lightning impulse waveforms - breakdown characteristics for non-standard lightning impulse waveforms associated with disconnector switching surges -", vol. 15, no. 3, pp. 721–729, 2008.

[9] A.B. Glot, I.A. Skuratovsky, Non-Ohmic conduction in tin dioxide based varistor ceramics, Mater. Chem. Phys. 99 (2–3) (2006) 487–493.

[10] C.A. Christodoulou, V. Vita, V. Mladenov, L. Ekonomou, On the computation of the voltage distribution along the non-linear resistor of gapless metal oxide surge arresters, Energies 11 (11) (2018).

[11] P. Valsalal, S. Usa, K. Udayakumar, Importance of capacitance on metal oxide arrester block model for VFTO applications, IEEE Trans. Power Deliv. 26 (2) (2011) 1294–1295.

[12] J. He, Metal oxide varistors from microstructure to macro-characteristics. 2019.

[13] C.A. Christodoulou, V. Vita, G. Perantzakis, L. Ekonomou, G. Milushev, Adjusting the parameters of metal oxide gapless surge arresters' equivalent circuits using the harmony search method, Energies 10 (12) (2017).

[14] A. Bayadi, N. Harid, K. Zehar, and S. Belkhiat, "Simulation of metal oxide surge arrester dynamic behavior under fast transients", Int. Conf. power Syst. transients, vol. 1, no. 1, p. 06 p, 2003.

[15] F. Fernández and R. Díaz, "Metal-oxide surge arrester model for fast transient simulations", pp. 0–4, 2001.

[16] M. Giannettoni, P. Pinceti, A simplified model for zinc oxide surge arresters, IEEE Trans. Power Deliv. 14 (2) (1999) 393–398.

[17] R.A. Jones, et al., Modeling of Metal Oxide Surge Arresters, IEEE Trans. Power Deliv. 7 (1) (1992) 302–309.

[18] V.S. Brito, G.R.S. Lira, E.G. Costa, M.J.A. Maia, A wide-range model for metal-oxide surge arrester, IEEE Trans. Power Deliv. 33 (1) (2018) 102–109.

[19] S.Ehsan Razavi, A. Babaei, Modification of IEEE model for metal oxide arresters against transient impulses using genetic algorithms, Aust. J. Basic Appl. Sci. 5 (10) (2011) 577–583.

[20] J. Lin, J. Zhang, J. Yang, High-voltage pulse generator based on magnetic pulse compression and transmission line transformer, Dig. Tech. Pap. Int. Pulsed Power Conf. (2013) 3–6.

[21] O.O. Melo, L.A. Lopez, and S.E. Melo, "Diseño de Experimentos: metodos y Aplicaciones", 2007.